Novel insights into the cold resistance of *Hevea brasiliensis* through coexpression networks

Carla Cristina Da Silva[1], Stephanie Karenina Bajay[1], Alexandre Hild Aono[1], Felipe Roberto Francisco[1], Ramir Bavaresco Junior[1], Anete Pereira de Souza[1,2], Camila Campos Mantello[3], Renato Vicentini dos Santos[4]*

[1]Molecular Biology and Genetic Engineering Center (CBMEG), University of Campinas (UNICAMP), Campinas, SP, Brazil

[2]Department of Plant Biology, Biology Institute, University of Campinas (UNICAMP), Campinas, SP, Brazil

[3]Hazera Seeds B.V., Warmenhuizen, The Netherlands

[4]Department of Genetics, Evolution, Microbiology and Immunology, Biology Institute, University of Campinas (UNICAMP), Campinas, SP, Brazil

*** Correspondence:**
Renato Vicentini dos Santos
shinapes@unicamp.br

Number of Words:10,851

Number of Figures: 4

Number of Tables: 1

Keywords: Breeding Strategies, Cold Stress, Edaphoclimatic Adaptation, Heuristic Cluster Chiseling Algorithm, RNA-Seq, Rubber Tree, Stress Gene Modules

Abstract

Hevea brasiliensis, a tropical tree species from the Amazon rainforest, is the main source of natural rubber worldwide. Due to the high pressure of fungal diseases in hot, humid regions, rubber plantations have been moved to "escape areas", which are dryer and have lower temperatures during the winter. Here, we combined gene expression data of a primary (GT1) and a secondary (RRIM600) young rubber tree clones, which present different cold tolerance strategies, to analyze rubber tree gene expression regulation during 24 h of cold exposure (10°C). Together with traditional differential expression approaches, a RNA sequencing (RNA-seq) gene coexpression network (GCN) comprising 27,220 genes was established in which the genes were grouped into 832 clusters. In the GCN, most of the rubber tree molecular responses to cold stress were grouped in 26 clusters, which were divided into three GCN modules: a downregulated group comprising 12 clusters and two upregulated groups comprising eleven and three clusters. Considering the three modules identified, the general *Hevea* response to short-term cold exposure involved downregulation of gibberellin (GA) signaling, complex regulation of jasmonic acid (JA) stress responses and programmed cell death (PCD) and upregulation of ethylene responsive genes. The hub genes of the cold-responsive modules were subsequently identified and analyzed. As a result of the GCN strategy applied in this study, we could not only access individual DEGs related to the *Hevea* cold response, but also provide insights into a deeper cascade of associated mechanisms involved in the response to cold stress in young rubber

trees. Our results may represent the genetic stress responses of the species, developed during its evolution, since the varieties chosen for this work are genotypes that were selected during the early years of rubber tree domestication. The understanding of *H. brasiliensis* cold response mechanisms can greatly improve the breeding strategies for this crop, which has a narrow genetic base, is impacted by climate change and is the only source for large-scale rubber production.

1 Introduction

Hevea brasiliensis, mainly known as rubber tree, is an allogamous perennial tree species native to the Amazon rainforest and belonging to the Euphorbiaceae family (Priyandarshan and Clément-Demange, 2004). Although rubber trees are the main source of natural rubber worldwide (Pootakham et al., 2017; Gonçalves and Fontes, 2009; De Faÿ and Jacob, 1989), this tree species is a recent crop and is still in domestication (Priyadarshan and Clément-Demange, 2004). The dispersal and domestication of rubber trees worldwide is based on only approximately 20 seedlings that were introduced in Southeast Asia in the late 19th century. These seedlings were the only survivors of a collection of thousands of seeds from the Amazon Basin, originating the selection of elite trees and controlled hybridization. Thus, until the present day, almost all commercial varieties of *H. brasiliensis* are derived from these seedlings; therefore, their genetic variability is quite narrow (Gonçalves and Fontes, 2009; Souza et al., 2015).

Although the Amazon Basin provides ideal conditions for rubber tree cultivation, the occurrence of fungal South American Leaf Blight (SALB) disease in the region hinders the establishment of rubber tree plantations in the area. To overcome this situation, Brazilian rubber tree plantations were moved to suboptimal areas (or "escape areas"), such as the Brazilian central and southeastern regions, which are dryer and present lower temperatures during the winter (Priyadarshan et al., 2009). Southeast Asian countries, whose climate conditions are similar to those of the Amazon and successfully avoided the introduction of SALB, are the major rubber producers worldwide. Nevertheless, these Asian plantations have already suffered heavy losses because of other fungal disease outbreaks (Priyadarshan and Gonçalves, 2003; IRCo, 2019; Pornsuriya et al., 2020) and have expanded to suboptimal areas as well, such as southern China and northeastern India (Priyadarshan et al., 2009). Thus, rubber tree varieties adapted to areas with new edaphoclimatic conditions are of key interest.

Among the stressing factors characteristic of escape areas, low temperatures heavily affect *H. brasiliensis* development, causing damage to leaves and latex production (Priyadarshan et al., 2005). For rubber tree plantations, prolonged low-temperature periods or frost occurrence can result in plant death (Priyadarshan et al., 2009). Cold stress triggers a massive reprogramming of gene expression in plants such that their metabolic processes are altered to cope with the cold environment (Theocharis et al., 2012). To promote breeding of cold tolerance in *H. brasiliensis*, a more in-depth understanding of the cold response mechanisms of this species is necessary.

In recent years, due to the impact of low temperatures in rubber tree plantations and rubber production, there has been an increase in the number of studies about *H. brasiliensis* molecular cold stress responses. The CBF-regulon genes *HbCBF1*, *HbICE1* and *HbICE2* have been identified and characterized, and their overexpression enhances cold tolerance in Arabidopsis (Cheng et al. 2015, Yuan et al. 2017, Chen et al. 2019). Long periods of low temperatures induce the demethylation of rubber tree cold-responsive gene promoters, while hypermethylation is observed during warmer periods (Tang et al. 2018). Jasmonic acid (JA) has been shown to modulate and enhance *Hevea* cold tolerance (Deng et al. 2018a, Chen et al. 2019), and cold-tolerant clones exhibit the upregulation of

calcium (Ca2+) signaling-related genes and reactive oxygen species (ROS)-scavenging enzymes. Through comparative genomics involving cold-resistant and cold-sensitive clones, thousands of differentially expressed genes (DEGs) have been identified in response to cold stress (Cheng et al. 2018, Deng et al., 2018, Mantello et al., 2019). Although such works have brought a wealth of information regarding the rubber tree molecular cold stress response, how these mechanisms come together and orchestrate this response needs to be better understood. Recently, Ding et al. (2020) modeled a gene coexpression network (GCN) and associated a network module in response to cold treatment. Although the cold response mechanisms were not assessed, the created GCN represents a rich source of data for investigating cold responses.

Here, we carried out a study based on a GCN modeled with combined transcriptomic data from two of the earliest *H. brasiliensis* clones to identify novel patterns between the genes involved in the species response to cold stress. The GCN use of the transcriptome data from a cold stress experiment with these genotypes, one resistant (RRIM600) and one tolerant (GT1), allowed the analysis of highly associated genes and their classification into clusters, some of which were enriched for different biological processes. Three main cluster modules for rubber tree cold stress response were delimited, which enabled the identification of central genes in the created networks underlying cold stress in rubber tree. This study aimed to provide insights on how this species copes with low temperatures by the use of clones with distinct cold response strategies and that are part of the basis of rubber tree domestication and breeding processes. This work is one of the pioneering works in determining the association of the molecular mechanisms of *Hevea* through GCNs and is the first to present rubber tree cold stress response mechanisms as an integrated network.

2 Material and Methods

2.1 RNA Sequencing (RNA-Seq) Experiments

The RNA-seq experiment was based on two clones of *H. brasiliensis* recommended for escape areas (Mantello et al., 2019): RRIM600 and GT1. Under low temperatures, RRIM600 presents an avoidance physiological strategy, while GT1 employs a balance between photosynthetic/growth activities and stress responses (Mai et al., 2010; Mantello et al., 2019). Raw RNA-seq data generated by Campos Mantello et al. (2019) (BioProject, PRJNA483203; Sequence Read Archive (SRA), SRX4491391-SRX4491414) were used for the analyses of the present work. The cold experiment consisted of exposing three six-month-old plantlets of each clone, which were provided by the Seringueira Center, Votuporanga, São Paulo, Brazil, to a temperature of 10°C for 24 h (12 h light/12 h darkness). During this period, sampling was carried out for each biological replicate by random collections of one green leaf at the mature stage, at 0 h (0h, control), at 90 mins (90m), at 12 h (12h), and at 24 h (24h) post-treatment. The RNA extracted from these samples was used to construct 24 cDNA libraries (three replicates of each clone for each time points).The 24 samples were randomly pooled (four samples per pool) and clustered using the TruSeq PE Cluster Kit on the cBot platform (Illumina, Inc., San Diego, CA, USA). The samples were sequenced using an Illumina Genome Analyzer IIx with the TruSeq SBS 36-Cycle Kit (Illumina, Inc., San Diego, CA, USA), for 72 bp paired-end (PE) reads.

2.2 Bioinformatics and Differential Gene Expression Analysis

The reads of each library considering their time points and genotypes' biological replicates were mapped with Bowtie2 v.2.2.6 (Langmead & Salzberg, 2012) to the reference transcriptome. The estimated abundance of reads for each sample was calculated by RSEM v.1.2.28 (Li & Dewey, 2011) using a Trinity accessory script (align_and_estimate_abundance.pl). Subsequently, a matrix

was constructed with expression values and abundance estimates between samples and replicates. Genes with a minimum of 10 counts per million (CPM) in at least three samples were kept for further analyses. These samples were normalized by the quantile method and transformed into log2cpm by the edgeR v.3.34.1 package (Robinson et al., 2010)

To explore the data and verify the behavior of the samples a principal component analysis (PCA) was performed in R (R Core Team 2020) using a singular value decomposition from the standardized log2cpm data (Z-score normalization). For DEG analysis, the datasets from GT1 and RRIM600 were combined in an attempt to create a unique *H. brasiliensis* expression dataset. An empirical Bayes smoothing method implemented in the edgeR v.3.34.1 package (Robinson et al., 2010) was used to identify differentially expressed genes (DEGs) between the time points sampled. The eBayes function with a minimum ratio of 0.01 was used to determine whether a gene is differentially expressed. The following comparisons were performed: (i) 0h vs. 90m; (ii) 0h vs. 12h; (iii) 0h vs. 24h; (iv) 90m vs. 12h; (v) 90m vs. 24h; and (vi) 12h vs. 24h. The p-values were adjusted using a Bonferroni correction, and genes for which the p-value was ≤ 0.05 were considered DEGs.

The identified DEGs were compared between the time points with Venn plots, which were constructed with the Venn R package (Dusa, 2017). For all genes, we selected the respective annotation obtained with the Trinotate v2.0.1 pipeline (Bryant et al., 2017; https://github.com/Trinotate/Trinotate.github.io). Transcripts were queried against the SwissProt/UniProt database using BLASTX (e-value of $1e^{-5}$), and placed into a tab-delimited file. Transcripts were also associated with Gene Ontology (GO) terms (Harris et al., 2004).

2.3 GCN Analysis

The GCN was inferred through R Pearson correlation coefficients with a cutoff of 0.8 (Van Noort et al., 2004). The R values of the GCN were normalized using the highest reciprocal rank (HRR) approach (limited to the top 10 connections), and the heuristic cluster chiseling algorithm (HCCA) was used to organize the network into communities (Mutwil et al., 2010). The HRR networks and the HCCA results were subsequently visualized with Cytoscape software v.3.8.0 (Shannon et al., 2003).

2.4 Cold Stress Association

The number of DEGs in the clusters was used to pinpoint the most likely groups involved in the *Hevea* cold stress response. Hub genes in the selected clusters were analyzed using the node degree distribution (DD), betweenness centrality (BC) and stress centrality (SC) distribution parameters of the networks obtained using Cytoscape software v.3.8.0 (Shannon et al., 2003). Genes that had a high DD and that presented high values of BC and SC were considered highly influential in the selected clusters' coexpression dynamics. For each selected network cluster, at least one hub gene was identified, and they were evaluated according to their functional annotation and/or according to the genes with which they interacted.

2.5 Functional Enrichment

Overrepresented GO terms in the clusters were determined with the BiNGO plugin v.3.0.4 (Maere et al., 2005) using a customized reference set created from the transcriptome annotation data. A hypergeometric distribution and false discovery rate (FDR) < 0.05 were used for the analyses. GO enrichment analyses were performed with EnrichmentMap plugin v.3.3.1 (Merico et al., 2010) with

FDR Q-values < 0.05 and the BiNGO output files. Both plugins were used in Cytoscape software v.3.8.0 (Shannon et al., 2003).

3 Results

3.1 Bioinformatics and Differential Expression Analysis

Approximately 530 million PE reads were obtained for the RRIM600 genotype, and 633 million were obtained for the GT1 genotype. After quality filtering, approximately 933 million PE reads were retained and used to assemble the transcriptome via the Trinity software. A total of 104,738 isoforms (51,697 genes) were identified, with sizes between 500 bp and 22,333 bp, with an average of 1,874 bp and N50 of 2,369. From these genes, we identified a total of 74,398 unique proteins related to 9,417 different GO terms (Supplementary Table 1).

The transcriptome data used were validated by Mantello et al. (2019). In addition to the validation of this RNA-seq data, genes that were analyzed by Silva et al. (2014) are also present in the network. Since qPCR experiments have already been performed by those who produced the data to validate the quantitative transcription data, we consider the data to be reliable for our analyses.

For DEG analyses, we employed a filtering criteria based on genes that presented at least 10 counts per million (CPM) in at least three samples, which resulted in a final number of 30,407 genes. From these genes, the PCA revealed a distinct profile of samples belonging to each different genotype (Figure 1A).

The number of DEGs per time period comparison showed different responses regarding not only the number of DEGs (Table 1) but also the associated genes (Supplementary Table 2). Although there was evident overlapping among the results (Figure 1B), a joint mechanism involving several genes for the cold response was clearly observed. We detected contrasting numbers of DEGs for the conditions established, with the highest number of DEGs identified at 0h and 24h and the smallest at 12h and 24h. Approximately 93% of the downregulated genes and 96% of the upregulated genes were annotated. Regarding the GO enrichment analysis, the full DEG set was enriched for response to stress and response to chitin terms. The downregulated group of genes did not present any overrepresented category. In contrast, the upregulated gene group was enriched for the following terms: response to chitin, defense response, response to wounding, cell death, photoprotection, calcium ion transmembrane transporter activity and integral to plasma membrane.

After 90 minutes of cold treatment, only thirty-two transcripts were characterized as DEGs, all of which were upregulated during the plantlets' early response to cold stress. Of these, 26 genes were successfully annotated (Supplementary Table 1). The annotated DEGs are known to be induced by cold as well as other abiotic stressors, such as drought and salt stresses. These DEGs are involved with cell wall tightening processes, growth inhibition, oxidative stress protection, calcium (Ca2+) signaling and cold-induced RNA processing. The late response, considered as the interval between twelve hours and 24 hours of cold treatment, contained 18 DEGs, including genes that stimulate an increase in the membrane diffusion barriers and cell wall modifications.

One hundred and thirty-eight DEGs were annotated with the GO term DNA-binding transcription factor activity, 103 of which were upregulated and 35 were downregulated. All of them except one were grouped in the cold stress response gene clusters (see below). An analysis of overrepresented GO terms for the 138 DEGs showed that they are involved with the regulation of cellular metabolic

processes: negative and positive regulations are modulated by the up- and downregulated groups, respectively. While the upregulated genes are responsive to stress and other stimuli, the downregulated genes promote plant development and growth. All transcripts annotated as members of the Apetala2/Ethylene-responsive factors (AP2/ERF) family and that were identified as DEGs (38) were upregulated. DEGs annotated as transcriptional repressors of JA-mediated responses (i.e., TIFY/JAZ proteins) were also upregulated.

Nonspecific serine/threonine protein kinases (EC: 2.7.11.1) were the most represented enzymes among the annotated DEGs: 165 were up-regulated while 57 were down-regulated. The up-regulated DEGs have an overrepresentation of GO terms related to reproduction processes, response to abscisic acid (ABA) stimulus, calmodulin binding and signal transmission, while the downregulated DEGs were enriched for posttranslational protein modification. The second most differentially expressed enzyme types were RING-type E3 ubiquitin transferases (EC: 2.3.2.27), with 42 and 11 genes up- and downregulated, respectively.

Among the annotated DEGs, four transcripts similar to Gibberellin 20 oxidase (GA20ox) protein, which belongs to the GA biosynthesis pathway, were downregulated. Transcripts similar to Allene oxide cyclases (AOC) and synthases (AOS) and Linoleate 13S-lipoxygenase (LOX), which synthetize oxylipins (i.e., 12-oxo phytodienoic acid, 12-OPDA) that are precursors of JA, were upregulated. Nevertheless, DEGs annotated as enzymes that attenuate JA-mediated stress responses were also upregulated; these include IAA-alanine resistant 3 (IAR3) and Cytochrome P450 94C1 (CYP94C1), which catalyze the turnover of JA (Heitz et al. 2012, Widemann et al. 2013).

3.2 Rubber Tree GCN Analysis

From the transcriptome data of both genotypes, we modeled an HRR network in order to represent the cold response of rubber tree (Figure 2A). This network was composed of 27,200 nodes (genes) across 50,650 connections (edges) that were grouped into 832 gene clusters. Only the top 10 Pearson R correlation coefficients (considering a 0.8 cutoff) were retained for each gene, and disconnected genes were disregarded. The major connected component within the network is composed of 25,608 nodes (94.1%). There were also 626 components for the remaining 1,592 genes, with the number of nodes in each component ranging from two to eleven. To identify putative gene associations within the network structure, we analyzed the network with HCCA, which revealed 832 clusters (Figure 2B). From these sets of genes, 626 corresponded to the disconnected components (mean cluster size of ~3), and 206 corresponded to the core GCN structure (mean cluster size of ~124), comprising clusters with sizes ranging from 45 to 280 genes (Supplementary Table 3).

Figure 2 shows that the complete network of transcripts from the cold experiment has a large amount of highly correlated genes, confirming the efficiency of the transcription analysis method of GCNs. The central portion of the network has the major part of genes, whose expression was not significantly different, while right and left ends concentrate the majority of DEGs. However, part B of Figure 2 highlights a region of the network where most groups contain DEGs, in which up- and downregulated transcripts responsible for a significant part of the results are shared; this is also the region where we made most of the inferences. It is possible to see in this figure that one group of DEGs can reach another with few connections. Thus, although we have a clear picture of the DEGs separated in part A of the figure, it is possible to find a region of the network in which the correlation of up- and downregulated DEGs functioning in common processes that interfere with each other can be analyzed.

Supplementary Figure 1 (part B) also shows the topological structure that seems to be the core of the main architecture of the network. This is the structure we used to analyze the DEGS and biological functions among the correlated genes. In part A of the figure, only the condensed groupings of up- and down-regulated genes are shown, with almost no connection between them, and part B shows the subnetwork that we used for most of the inferences in this work, given the concurrent connectivity between up- and downregulated genes active in response to cold stress.

Functional coherence is expected across coexpressed genes belonging to the same cluster. As such, an enrichment analysis of GO terms was performed for each cluster of genes identified by the HCCA. From the 206 main clusters, 39 (14%) had GO terms that were significantly enriched, as highlighted in Figure 3 for biological process GO terms. Response to stress was the most overrepresented term among clusters, encompassing 1,039 genes across nine groups, which was expected considering the cold experimental design. Two of these clusters (c14 and c28) were also enriched for developmental processes, indicating the tight correlation between environmental stimuli and growth. Interestingly, we also observed seven clusters enriched for virus replication and transposition processes.

In addition to the clustering structure evaluated on the GCN topology, we also assessed the gene centrality measures (Supplementary Table 3). From the 27,220 genes in the network, only 507 had the maximum permitted connections (ten). One of them, annotated as "probable cytochrome c biosynthesis protein" (CCBS), also presents the highest values of SC and BC centralities, indicating that this gene exerts a great influence on the network. This gene belongs to cluster c8, which was enriched for photosynthesis, but also for cellular respiration and transposition processes. By evaluating the intercluster connections in the HCCA-based contracted network (Figure 3B and Supplementary Table 4), we found that the cluster with the highest number of connections is c117 (nine edges), which was enriched for developmental processes.

Figure 3 presents an important aspect of the network architecture, which returns similarity with the biological functions. According to the distribution of GO terms in the network architecture, it is possible to see enrichment of correlated pathways distributed in close groups in the GCN. This coherence between enrichment of correlated GO terms corroborates the application of this method as a valuable source of inferences.

3.3 Gene Clusters Mostly Related to the Cold Stress Response

Even though the DEGs identified were dispersed throughout the GCN (Figure 2A), specific patterns could be observed in several clusters. To identify molecular associations with the cold stress response, we selected the clusters that together accounted for 70.2% (1,751) of the DEGs identified. We considered as associated clusters those that contain at least 50% of their genes as DEGs (Supplementary Table 5), expanding the module across these clusters' neighbors considering a minimum required frequency of 20% of DEGs inside a cluster (Figure 3 and Supplementary Figure 1). Interestingly, we established three GCN modules for the 31 clusters selected: (i) a downregulated group with 12 clusters, (ii) an upregulated group with 11 clusters, and (iii) an upregulated group with three clusters. Even though there were additional clusters with DEGs, only the most pronounced clusters were used for novel inferences.

293 Among the DEGs in the selected clusters, 480 were annotated with enzyme code (EC) numbers,
294 being 339 up-regulated and 141 down-regulated transcripts. Moreover, 180 DEGs were assigned to
295 KEGG pathways. Cold exposure triggered the upregulation of transcripts similar to enzymes
296 involved in the synthesis of zeaxanthin and lutein (c106) and lipoic acid (lipoamide) (c194). Several
297 enzymes from the nucleotide sugar metabolic pathway were upregulated (c101, c106, c121, c130,
298 c143, c16, c161, c34, c53). Enzymes in the methionine metabolism pathway that produce ethylene as
299 their final product were also upregulated (c121, c28, c34), as well as α-linolenic acid metabolism
300 enzymes that synthetize oxylipins (c126, c159, c34, c53) and enzymes that promote the turnover of
301 JA (c194, c53).

302 The module of downregulated genes (i), as a whole, did not present any overrepresented GO term
303 category. This module bears transcripts similar to Gibberellin receptor GID1C protein (clusters c153
304 and c196), which is a positive regulator of GA-signaling (Griffiths et al. 2006). Together with the
305 downregulation of putative *GA20ox* transcripts in non-selected clusters, these results indicate that
306 rubber tree decreases GA-mediated processes during cold stress. Two transcripts annotated as
307 Coronatine-insensitive protein 1 (COI1), an F-box protein that promotes the degradation of JAZ
308 proteins (Thines et al. 2007), were also assigned to clusters in this module (c184 and c42).
309 Interestingly, members of the florigen *CONSTANS* gene family were downregulated and the DEGs
310 were associated to clusters c134, c184 and c48.

311 GO enrichment of module (ii) showed that signaling processes were amplified, since MAP kinase
312 kinase kinase (MAPKKK) and calcium ion (Ca^{2+}) transmembrane transporter activities were
313 overrepresented. The group was also enriched for response to stress, photoprotection and plant-type
314 hypersensitive response. Additionally, we also observed in (ii) clusters enriched for specific GO
315 terms. Twenty-five and three early-response genes were grouped into clusters c14 and c159,
316 respectively. c14 was the cluster with the most overrepresented GO categories among the groups of
317 the modules selected, being enriched for response to high-light intensity, response to ROS and
318 transcriptional regulation activity. Other clusters from this module were enriched for stress response
319 (c28, c126 and c159), ion transport (c34), development (c28) and translation (c143). Twenty-six of
320 the 38 DEGs annotated as AP2/ERF proteins and all DEGs annotated as JAZ proteins (8) were
321 assigned to the clusters of module (ii). In addition, five putative RING1 E3 ubiquitin-protein ligases,
322 which are involved in the regulation of programmed cell death (PCD) during the plant hypersensitive
323 response (Lin et al., 2008; Lee et al., 2011), were placed in clusters c14, c161 and c28. The two
324 transcripts from c14 are early-responsive genes, being upregulated after 90m of cold exposure.
325 Intriguingly, the second transcript with the highest BC and SC values in the whole network was in
326 cluster c28 and was not functionally annotated; this transcript has seven connections, four of which
327 with genes from different clusters. Its sequence is conserved among plant species and is described as
328 an uncharacterized protein.

329 The genes clustered in the second module of upregulated genes (iii), according to the enrichment
330 analysis, are mostly involved in carbohydrate metabolic processes, lipid phosphorylation and
331 phosphatidylinositol phosphate biosynthetic processes. By itself, cluster c106 was enriched for
332 developmental growth and water homeostasis.

333 The GO terms identified in the modules selected were summarized into several biological processes
334 and then separated into up- (Figure 4A) and downregulated (Figure 4B) categories. Although up- and
335 downregulated DEGs from these modules present evident similarities into terms of GO annotations,
336 it is clearly observed that the same biological processes are affected in specific ways.

To evaluate the importance of genes inside these modules, we evaluated the presence of central genes inside each cluster: the hub genes. The network structure allows the insertion of ten edges for each node while respecting the minimum Pearson correlation of 0.8; however, if a highly connected node has low BC and SC values, it was not selected as a hub. As such, this maximum number of connections was not observed in all the selected hubs. In total, 39 hub genes were identified in the selected clusters: 16 for module (i), 18 for module (ii) and five for module (iii). Among the hubs, there are transcripts similar to proteins involved in developmental processes, response to stress, uncharacterized proteins and three transcripts whose sequences were not similar to any sequence in the BLASTN Nt database. (Supplementary Table 6). A BLASTN search against other Euphorbiaceae species genomes returned no results. Thus, possibly, these sequences are specific at least to the genus. Interestingly, two hub genes from module (iii) were not among the set of DEGs.

4 Discussion

The optimal conditions for *H. brasiliensis* development are temperatures ranging from 22-30°C, relative humidity of 70% or higher, and annual rainfall between 1,500 and 3,000 mm. Considering the damage of low temperatures to rubber production, rubber tree breeding programs worldwide have been focusing on the development of genotypes with both high productivity and tolerance to cold stress present in escape areas. Thus, the work carried out in this paper, which starts from transcripts of genotypes that represent a good portion of the genomic makeup of commercial rubber tree clones, opened avenues for understanding the response to cold stress in the species.

GT1 is a primary clone obtained through open pollination of the wild seedlings introduced in Southeast Asia and their unselected progeny. RRIM600 was selected in the first rubber tree breeding cycle, when breeders first used controlled pollination. Both genotypes are prime progenitors of modern rubber tree clones (Priyadarshan et al., 2009). Considering the long life cycle of rubber trees and the low number of generations that have occurred, these clones are substantially close to their wild ancestors; therefore, they may be considered as genotypes bearing the wild *Hevea* natural genetic variation. . For this reason, we used these genotypes to make inferences concerning *H. brasiliensis* cold resistance.

We started our analyses by identifying genes modulated at different time points of cold exposure. The small number of responsive genes may indicate that the plants are able to withstand a few hours of cold exposure without massive activation or repression of genes. After twelve hours of exposure to the cold, we observed that the plantlets underwent a reprogramming in terms of their expression profiles (DEGs identified at 0h vs. 12h), with the new programming essentially being maintained for the next twelve hours (DEGs identified at 12h vs. 24h). Similar results were observed in rubber tree comparative transcriptome works as well (Cheng et al. 2018, Deng et al. 2018a, Mantello et al. 2019) and a higher number of DEGs was identified in the cold-tolerant genotypes (Cheng et al. 2018, Mantello et al. 2019). Our results indicate that the species, and not only selected clones, has a delayed response to low temperatures in terms of gene expression modulation.

In addition to DEG analyses, we constructed GCNs to expand our inferences concerning genes involved in the cold response. Analyses based on such a structure are a promising approach to better elucidate the participation of genes associated with cold stress. Considering that such tolerance is the result of a network of complex biochemical pathways, an appropriate way to understand such regulation is evaluating not a single gene but rather a set of associated genes corresponding to a broad molecular mechanism. As such, we did not search for specific genes inside the GCN; instead, the structure and connections of the GCN helped guide us to identify potential candidate genes and interactions that might play essential roles in the rubber tree cold stress response. The correlations of

how the coordinated expression of genes involved in multiple metabolic pathways act in unison can be elucidated through the definition of clusters within the GCN (Umer et al, 2020; Sun et al., 2021). Recently, using several public rubber tree transcriptomes, Ding et al. (2020) modeled a GCN, providing insights into rubber biosynthesis. Even with high potential, such approaches are still relatively new in rubber tree research, and this study is the first initiative on evaluating *Hevea* cold response from a more holistic perspective.

4.1 Selection of Cold Response-Associated Clusters

From the GCN clusters selected as being associated with the rubber tree cold stress response, analysis of enzymes and correspondent metabolic pathways led to the identification of potential cold-related metabolic changes. Enzymes involved in the synthesis of protective photosynthetic pigments (i.e., zeaxanthin and lutein) (Dall'Osto et al., 2006) and lipoic acid (lipoamide), which protects against oxidative stress (Navari-Izzo et al., 2002), were upregulated. Nucleotide sugars are essential for cell wall biosynthesis and can function as signaling molecules, being sugar donors for the targeted-glycosylation of different compounds (Figueroa et al., 2021). The GCN indicates that ethylene biosynthesis is correlated with nucleotide sugar pathway enzyme expression (c121, c34) as well as the synthesis of oxylipins (c34). Oxylipins are synthetized in the plastids and then are transported to the peroxisomes for the synthesis of JA. These molecules have signaling functions, working independently from JA in response to stresses (Du et al., 2013; Maynard et al., 2018; Wang et al., 2020). JA mediates rubber tree response to cold stress, nonetheless cold-tolerant clones promote the downregulation of *COI1* while *JAZ* genes are upregulated (Deng et al. 2018a). Taken together, our results suggests that the primary rubber tree strategy might be employing OPDAs as signals to trigger short-term cold responses rather than JA, which might be transiently used in specific periods.

MAPK and Ca^{2+}-signaling processes increased during cold exposure. This mechanism of action in response to cold stress has been reported in other studies, where several metabolites were found to act as low-temperature sensors; in response cells release calcium through phosphatidylinositol signaling and inositol phosphate metabolism through the MAPK signaling pathway. This MAPK signaling pathway in turn triggers signal transduction via transcription factors (TFs) such as ERFs, bHLHs and MYBs (Sun, 2021). Mantello et al. (2019) detected the upregulation of transcripts similar to Calmodulin-like proteins (CML) in rubber tree during cold stress in both RRIM600 and GT1 genotypes. Here we also identified several upregulated transcripts annotated as CMLs and Calcium-dependent protein kinases (CDPKs), and the central cluster of module (ii) (c34) was enriched mainly for cellular Ca^{2+} flux processes, indicating that Ca^{2+}-signaling has a major role in rubber tree cold response. Cheng et al. (2018) observed an upregulation of *MAPK* and *MAPKKK* genes both in the cold-tolerant (CATAS93-114) and in the cold-susceptive (Reken501) clones; however, the expression of *MAPKKK* genes was higher in the tolerant genotype. Accordingly, our results demonstrate that the MAPKKK signaling cascade is enhanced in rubber trees under low temperature stress and that it seems to be a *H. brasiliensis* basal line of defense against the cold environment.

The starting point of the rubber tree cold stress response mainly lies in cluster c14, which harbors several sequences annotated as *ethylene-responsive transcription factors* (*ERFs*). *ERFs* are activated by the ethylene signaling pathway and regulate the transcription of ethylene-responsive genes, which negatively impact plant growth (Müller and Munné-Bosch, 2015; den Broeck et al., 2017). The *ERF* TF family in rubber tree comprises 115 members (Duan et al., 2013), and the overexpression of an Arabidopsis *ERF1* ortholog in rubber tree plants enhanced their tolerance to abiotic stresses and augmented laticifer cell differentiation (Lestari et al., 2018). The rubber tree ERF genes expression is modulated by low temperature, either up- or downregulated (Gong et al. 2018). Deng et al. (2018a) observed that a cold-tolerant clone downregulated genes that promoted ethylene-signaling,

428 suggesting that the cold-tolerant clone repressed the ethylene-mediated response during cold stress.
429 In our analysis, all DEGs annotated as genes encoding ERFs were upregulated, suggesting that *H.*
430 *brasiliensis* plantlets maintained the ethylene-mediated stress response activity during the whole
431 experiment. The upregulation of ethylene biosynthesis-related enzymes also indicates that ethylene
432 might have a primary role in the rubber tree cold stress response.

433 In addition to being enriched for response to stress and protein ubiquitination, cluster c159 has
434 transcripts annotated as ERFs, calmodulin binding proteins, serine/threonine protein kinases and
435 disease-responsive genes. c159 also harbors two *BON1-associated protein 2* (*BAP2*) genes, one being
436 an early-responsive gene. BAP proteins are negative regulators of cell death in plants, which is
437 essential for plant development and the hypersensitive response, and *BAP* expression is modulated by
438 temperature (Yang et al., 2007; Cao et al., 2019; Hou et al., 2018).

439 Cluster c143 was enriched for the translation process, more specifically for negative regulation of
440 translation. This group contains three members of the *Carbon Catabolite-Repressor 4* (*CCR4*)-
441 *associated factor 1* (*CAF1*) gene family that were upregulated in response to cold treatment. These
442 deadenylase proteins promote translation suppression and mRNA degradation (Collart 2016, Fang et
443 al., 2020). In plants, CAF1 proteins were shown to be necessary for proper development and stress
444 response processes (Sarowar et al., 2007; Liang et al., 2009; Walley et al., 2010; Shimo et al., 2019;
445 Fang et al., 2020, 2021; Wang et al., 2021). In addition, stress-responsive TFs, nucleotide sugar
446 biosynthesis-related enzymes and cell wall biogenesis proteins, were assigned to cluster c143.

447 In addition to being enriched for stress responses and developmental processes, the GO terms
448 "positive regulation of protein kinase activity" and "DNA-binding transcription factor activity" were
449 overrepresented in cluster c28. Among the 108 transcripts that were functionally annotated, 25 (23%)
450 are TFs involved in the regulation of the plant defense response. The most represented TF family in
451 this cluster was the WRKY family, with eight members. WRKY TFs are one of the largest plant-
452 specific TF families, and they participate in the regulation of plant growth and development as well
453 as promote plant stress response by activating and inhibiting target gene transcription and modulating
454 signaling cascades (Jiang et al., 2017). Cluster c28 also harbors transcripts similar to calmodulin-
455 binding proteins and small auxin upregulated RNA (SAUR) proteins, which are essential growth
456 factors for regular plant development and adaptive growth under stress conditions (Stortenbeker and
457 Bemer, 2019; He et al., 2021). In rubber tree, the expression of a SAUR gene was higher in a cold-
458 tolerant clone, which also downregulated auxin signaling genes (Deng et al. 2018a). In addition, this
459 cluster has a strong candidate for further analysis of the rubber tree cold stress response:
460 PASA_cluster_65283, the uncharacterized protein with the second highest BC and SC values in the
461 whole GCN. Some of its connected transcripts were annotated as proteins involved in different
462 mechanisms in plant stress responses, such as the JA-dependent defense response and Ca^{2+} signaling.

463 Another cluster that also showed enrichment for stress responses was cluster c126, with an
464 overrepresentation of GO terms for phenylalanine biosynthesis and sphingolipid biosynthesis
465 processes. Phenylalanine, apart from its role in protein biosynthesis, is the precursor of several plant
466 phenolic compounds, such as lignin, flavonoids, anthocyanins (Maeda and Dudareva, 2012), and
467 salicylic acid (SA) (Lefevere et al., 2020). Sphingolipids constitute a significant part of plant plasma
468 membrane lipids and are also involved in the control of PCD and the mediation of SA signaling in
469 the plant stress response (Pata et al., 2010; Alden et al., 2011; Rivas-San Vicente et al., 2013).

470 In module (ii), cluster c34 is the main player in Ca^{2+} signaling and is enriched for transmembrane
471 transport of Ca^{2+}, which controls Ca^{2+} influx. Ca^{2+} is widely known as a secondary messenger in
472 plants (Zhu, 2016; Yuan et al., 2018; Michailidis et al., 2020). Low temperature stimuli is well

473 known to be a main trigger of cell Ca^{2+} influx through the activation of Ca^{2+} channels, which leads to
474 a Ca^{2+}-signaling cascade of plants in response to cold stress (Mori et al., 2018; Liu et al., 2021; Mao
475 et al., 2021).

476 The remaining five clusters in module (ii) did not present any overrepresentation of GO terms in the
477 enrichment analysis; nevertheless, the genes present in these clusters are involved in signaling
478 processes, response to stress and transcriptional regulation. *H. brasiliensis* has 18 *JAZ* genes (Chao et
479 al. 2019), and four DEGs annotated as *TIFY*/*JAZ* TFs were assigned to cluster c53. The *TIFY*/*JAZ* TF
480 family is specific to plants, and its members are negative regulators of JA-induced responses.
481 Nevertheless, their expression is induced by JA, which creates a regulatory feedback loop for fine-
482 tuning JA signaling (Chini et al., 2007). Exogenous methyl jasmonate induces latex biosynthesis
483 (Deng et al. 2018b), and some rubber tree *JAZ* members are involved in the regulation of laticifer
484 differentiation and rubber biosynthesis (Deng et al. 2018b, Chao et al. 2019).

485 Cluster c101 has a putative gene that encodes BAM1, a receptor protein kinase involved in plant
486 development (DeYoung et al., 2006) and is required for long-distance signaling for stomatal closure
487 (Takahashi et al., 2018). c101 also houses a transcript similar to the DELLA protein RGL1, which is
488 a negative regulator of the growth-promoting phytohormone gibberellin (GA) signaling pathway
489 (Wen and Chan, 2002). Poplar plants overexpressing this gene showed severe dwarfed phenotypes
490 (Busov et al., 2006). This cluster also contains a regulator of PCD. *Myb108* is a negative regulator of
491 ABA biosynthesis and ABA-induced cell death (Cui et al., 2013) and is highly induced in rose plants
492 under chilling (4°C) and freezing (-20°C) treatments. Compared with wild-type Arabidopsis plants,
493 Arabidopsis plants overexpressing the rose *Myb108* ortholog showed improved cold tolerance and
494 better performance under other stresses as well as a shorter growth cycle (Dong et al., 2021).

495 The cluster with the most enzymes mapped to the KEGG pathways was c121, with forty-four
496 transcripts assigned to EC numbers. Enzymes that synthesize scopolin and lignins in the
497 phenylpropanoid biosynthesis pathway were placed in this cluster. The coumarin scopolin and its
498 precursor, scopoletin, accumulate in plant tissues in response to stress (Kai et al., 2006; Zandalinas et
499 al., 2017) and are believed to be involved in ROS scavenging (Chong et al., 2002; Lee et al., 2013).
500 Members of the plant ACT domain-containing protein family (ACR4 and ACR8) are present in
501 cluster c161, and their expression is induced by cold treatment in Arabidopsis (Hsieh and Goodman,
502 2002). Regarding PCD, c161 harbors proteins that positively (the E3 ubiquitin-protein ligase RING1)
503 or negatively (Accelerated cell death 11 (ACD11)) regulate cell death. The expression of *RING1* is
504 induced by biotic stress, and the protein is necessary for the activation of PCD (Lin et al., 2008; Lee
505 et al., 2011). ACD11 is a sphingolipid transfer protein that controls cell death through the regulation
506 of sphingolipid levels (Brodersen et al., 2002; Simanchu et al., 2014). It is downregulated by the UPS
507 machinery after pathogen infection (Liu et al., 2017); however, ACD11 transiently accumulates in
508 response to low concentrations of ABA and under salt and drought stresses, and its overexpression
509 confers abiotic stress tolerance to plants (Li et al., 2020).

510 Cluster c194 contains proteins involved in the negative regulation of SA-mediated PCD (the MACPF
511 domain-containing proteins CAD1 and NSL1) (Tsutsui et al., 2006, Noutoshi et al., 2006), regulation
512 of photoperiod gene expression and the circadian clock (the WD repeat-containing protein LWD1)
513 (Wu et al., 2008; Wang et al., 2011), sugar transporters involved in cell wall biogenesis (UDP-
514 galactose transporter 2) (Norambuena et al., 2005), and plant growth and stress responses (Sugar
515 transport protein 13) (Schofield et al., 2009; Lee and Seo 2021), in addition to containing lignin-
516 synthesizing proteins.

517 **4.2 Identification of Key Elements within Cold Response-Associated Modules**

518 In addition to evaluating the functional profiles of all the associated genes within the modules
519 selected, we inferred about the importance of these genes in terms of the cold response mechanism.
520 Genes with high centrality within a GCN may be described as core regulators (Amrine et al., 2015),
521 which are known as hubs. Through the criteria defined for selecting hubs, we could identify hub
522 genes for each cluster of the cold stress gene modules, which are considered key elements in the
523 definition of cold resistance (Carlson et al., 2006; Koido et al., 2018).

524 Thirty-seven of the 39 identified hub genes were identified as DEGs, and 36 were successfully
525 annotated (Supplementary Table 6). The annotated hubs indicate that downregulation of
526 photosynthesis, ABA signaling, inhibition of growth and, interestingly, genes involved in the
527 flowering process are central to *H. brasiliensis* short-term cold response. In addition, the three
528 unannotated hubs apparently are sequences that are specific to rubber tree, which makes them
529 interesting targets for further research into their functions in *H. brasiliensis* cold stress response.

530 The functional annotation of two of these hubs indicated a downregulation of photosynthetic pathway
531 genes (clusters c42 and c166). The c42 hub gene was annotated as lycopene beta cyclase
532 chloroplastic/chromoplastic (LCYB), an enzyme of the carotenoid biosynthesis process. Carotenoids
533 form pigment-protein complexes in photosystems, protecting the machinery from ROS generated by
534 abiotic stresses (Dall'Osto et al., 2014; Shi et al., 2015; Kang et al., 2018). The hub gene from cluster
535 c166 was annotated as OTP51, a pentatricopeptide repeat-containing protein that is required for the
536 proper assembly of photosystems I and II in Arabidopsis and rice (de Longevialle et al., 2008; Ye et
537 al., 2012). Combined with low temperature, light promotes an enhancement in the transcription of
538 cold-responsive and photosynthesis-related genes (Soitamo et al., 2008). The downregulation of both
539 hub genes in rubber trees might be linked to the reduction in photosynthetic activity due to cold
540 stress; nevertheless, this modulation was detected in the dark period of the experiment.

541 Two hub genes were annotated as proteins involved in ABA signaling, which is essential for
542 development and responses to abiotic stress. A transcript similar to a protein phosphatase 2C (PP2C)
543 is one of the hubs in cluster c171. Chao et al. (2020), in a genome-wide identification and expression
544 analysis of the phosphatase 2A family in rubber tree, identified cis-acting elements related to low
545 temperature responsiveness (LTR). Under nonstress conditions, PP2C proteins were shown to
546 negatively regulate the ABA-mediated signaling pathway by inactivating ABA-responsive genes.
547 Once plants are under stress, ABA receptors bind PP2Cs and inhibit their activity, consequently
548 activating ABA signals (Cai et al., 2017). A cold-tolerant rubber tree genotype (CATAS93-114) also
549 downregulated PP2C genes while under cold stress (Deng et al. 2018). The other hub gene belongs to
550 cluster c134 and was annotated as zinc finger CONSTANS-like 4 protein (COL4), a TF. COL4 is a
551 flowering inhibitor that represses *flowering locus T* (*FT*) gene expression (Steinbach, 2019), and
552 strikingly, it is also involved in abiotic stress responses through the ABA-dependent signaling
553 pathway in Arabidopsis (Min et al., 2014). Considering that the ABA concentration might have
554 increased in the rubber trees during cold exposure, which is enforced by the downregulation of a
555 transcript similar to a PP2C protein, one could expect that this gene would be upregulated instead.
556 ABA is known to delay flowering; nevertheless, under severe drought conditions, ABA upregulates
557 florigen genes, which is part of the drought escape (DE) strategy. DE prompts plants to accelerate
558 their vegetative growth and reproduction stages during the high–water availability period. During the
559 drought season, these plants enter a dormant stage (Verslues and Juenger 2011; Yildirim and Kaya
560 2017).

561 The hub gene from cluster c156 was annotated as histone acetyltransferase of the MYST family (HAM)
562 1/2 proteins, which are involved in UV-B DNA damage repair (Campi et al., 2012). In Arabidopsis,

563 HAM1 and HAM2 proteins are expressed mainly in growing tissues and double mutants are lethal
564 (Latrasse et al., 2008). Interestingly, these proteins positively regulate the expression of *FLOWERING*
565 *LOCUS C* (*FLC*) gene, therefore, they are flowering repressors (Xiao et al., 2013). The downregulation
566 of this transcript in *H. brasiliensis* plantlets might be due to a decrease in DNA damage from UV-B
567 because of the absence of light. One of the hub genes for cluster c196 was annotated as Homeobox
568 protein BEL1 homolog, which is also involved with the flowering process. BEL1 controls ovule
569 integument identity and is required for auxin and cytokinin signaling for ovule development (Bhatt et
570 al. 2004, Bencivenga et al., 2012). The down-regulation of four genes from different metabolic
571 processes that are involved in the flowering process suggests that rubber tree may have a DE-type
572 strategy to deal with abiotic stresses.

573 The downregulation of three other strongly coexpressed hub genes from the c184, c171 and c153
574 clusters detected in the last timepoint of the cold experiment also suggests an increase in ABA
575 synthesis by the *H. brasiliensis* plantlets associated with growth inhibition and photoperiod. The hub
576 identified for cluster c184 was annotated as homeobox-leucine zipper (HD-Zip) protein HAT5
577 (AtHB1), and it was detected as a downregulated gene in rubber tree after 12h of cold exposure. HD-
578 Zip TFs seem to be a plant-specific TF family and its members take part in plant development and
579 stress responses (Ariel et al., 2007), with each member having its own expression pattern under
580 different environmental conditions (Li et al., 2019; Li et al., 2020). In Arabidopsis, *HAT5* expression
581 is downregulated in response to salt stress and low temperature; however, *HAT* expression is
582 upregulated in response to darkness (Henriksson et al., 2005), and the HAT protein acts as a positive
583 regulator of growth by modulating the expression of genes involved in cell elongation and cell wall
584 composition (Capella et al., 2015). This hub gene was connected to not only the c171 hub gene but
585 also to the c153 hub gene, which was annotated as leaf rust receptor-like kinase 10-like (LRK10L)
586 protein. LRK10 is a disease resistance gene first described in wheat (Feuillet et al., 1997), and
587 members of this family in wheat were shown to be induced by stress and light. Interestingly, in the
588 dark, these genes were downregulated even though the plants were under biotic stress (Zhou et al.,
589 2007). The homologous gene in Arabidopsis encode two different proteins: one is involved in ABA
590 signaling and is downregulated by drought stress and ABA treatment, while the other is upregulated
591 under these conditions, which indicates that these transcripts might regulate each other (Lim et al.,
592 2015). These three hub genes were strongly coexpressed together in rubber trees, directly connecting
593 three different clusters.

594 Considering the differences in the cold stress response of two *H. brasiliensis* clones obtained in the
595 early years of rubber tree domestication, we attempted to have a glimpse of the general genetic
596 processes of *Hevea* in response to cold stress. As a tropical tree species, rubber tree most likely did
597 not have to deal with prolonged periods of low temperature during its evolution; nevertheless, the
598 few wild genotypes that were successfully introduced in Southeast Asia carried so much genetic
599 diversity that breeding for varieties that are cold tolerant is still possible. As a result of the GCN
600 strategy applied in this study, we could visualize *Hevea*'s primary reprogramming of gene expression
601 and the relationship among the genes involved in the cold stress response. During the short period of
602 cold exposure used in this work, the plantlets activated the ethylene-mediated signaling pathway
603 since the beginning of the stress treatment, and ethylene signaling was active throughout the stress
604 period. PCD plays a major role in the rubber tree cold response process and is tightly regulated by
605 signaling cascades. Moreover, growth inhibition and cell wall thickening are implemented by the
606 plantlets, which may be associated with DE strategy triggered by cold stress. In view of the
607 genotypes analyzed, our results may represent the genetic stress responses developed during the

evolution of this species. The understanding of how *H. brasiliensis* copes with low temperature stress can greatly improve the breeding strategies for this crop species and emphasizes the importance of rubber tree genetic diversity preservation, since this species has such a narrow genetic base, it is impacted by climate change and is the only source for large-scale rubber production.

Conflicts of Interest

The authors declare that the research was conducted in the absence of any commercial or financial relationships that could be construed as potential conflicts of interest.

Author Contributions

AS, CS, CM and RV conceived the project, and CS, SB, AA, FF, RB and RV performed the analyses and wrote the manuscript. All authors reviewed, read and approved the manuscript.

Funding

The authors gratefully acknowledge the Fundação de Amparo à Pesquisa do Estado de São Paulo (FAPESP) for a PD fellowship to CS (2015/24346-9); Ph.D. fellowships to SB (2019/13452-3), AA (2019/03232-6), and FF (18/18985-7); and a master's fellowship to RB (2018/23831-9). In addition, the authors gratefully acknowledge Coordenação de Aperfeiçoamento de Pessoal de Nível Superior (CAPES) for financial support (Computational Biology Program - 88882.160095/2013–01) and for an internship fellowship to SB (PE-BOLSAS7349056) and the Conselho Nacional de Desenvolvimento Científico e Tecnológico (CNPq) for a research fellowship to AS (312777/2018-3).

627 **References**

628 Alden K P,Dhondt-Cordelier S, McDonald K L, Reape T J, Ng C K Y, McCabe P F, Leaver C J. (2011).
629 Sphingolipid long chain base phosphates can regulate apoptotic-like programmed cell death in
630 plants. Biochem Biophys Res Commun. 410(3):574-80. doi: 10.1016/j.bbrc.2011.06.028.

631 Amrine, K. C., Blanco-Ulate, B., & Cantu, D. (2015). Discovery of core biotic stress responsive genes
632 in Arabidopsis by weighted gene co-expression network analysis. *PloS one*, *10*(3), e0118731.

633 Ariel F D , Manavella P A, Dezar C A, Chan R L. (2007). The true story of the HD-Zip family. Trends
634 Plant Sci.12(9):419-26. doi: 10.1016/j.tplants.2007.08.003.

635 Bencivenga, S., Simonini, S., Benková, E., and Colombo, L. (2012). The transcription factors BEL1
636 and SPL are required for cytokinin and auxin signaling during ovule development in
637 Arabidopsis. Plant Cell 24, 2886–2897. doi: 10.1105/tpc.112.10016.

638 Bhatt AM, Etchells JP, Canales C, Lagodienko A, Dickinson H. (2004). VAAMANA--a BEL1-like
639 homeodomain protein, interacts with KNOX proteins BP and STM and regulates inflorescence
640 stem growth in Arabidopsis. Gene. 17;328:103-11. doi: 10.1016/j.gene.2003.12.033. PMID:
641 15019989.

642 Bryant DM, Johnson K, DiTommaso T, Tickle T, Couger MB, Payzin-Dogru D, Lee TJ, Leigh ND,
643 Kuo TH, Davis FG, Bateman J, Bryant S, Guzikowski AR, Tsai SL, Coyne S, Ye WW,
644 Freeman RM Jr, Peshkin L, Tabin CJ, Regev A, Haas BJ, Whited JL. (2017). A Tissue-
645 Mapped Axolotl De Novo Transcriptome Enables Identification of Limb Regeneration
646 Factors. Cell Rep. 17;18(3):762-776. doi: 10.1016/j.celrep.2016.12.063.

647 Cao Shifeng, Xiao Zeyu, Jiranek Vladimir, Tyerman Stephen D. (2019) The VvBAP1 gene is identified
648 as a potential inhibitor of cell death in grape berries. Functional Plant Biology 46:428-442.

649 Carlson, M. R., Zhang, B., Fang, Z., Mischel, P. S., Horvath, S., & Nelson, S. F. (2006). Gene
650 connectivity, function, and sequence conservation: predictions from modular yeast co-
651 expression networks. BMC genomics, 7(1), 1-15.

652 Chao J, Zhao Y, Jin J, Wu S, Deng X, Chen Y, Tian WM. (2019). Genome-Wide Identification and
653 Characterization of the JAZ Gene Family in Rubber Tree (Hevea brasiliensis). Front Genet.
654 2019 May 1;10:372. doi: 10.3389/fgene.2019.00372.

655 Chao J, Huang Z, Yang S, Deng X, Tian W (2020) Genome-wide identification and expression
656 analysis of the phosphatase 2A family in rubber tree (Hevea brasiliensis). PLOS ONE 15(2):
657 e0228219. https://doi.org/10.1371/journal.pone.0228219

658 Chen WJ, Wang X, Yan S, Huang X, Yuan HM. (2019). The ICE-like transcription factor HbICE2 is
659 involved in jasmonate-regulated cold tolerance in the rubber tree (Hevea brasiliensis). Plant
660 Cell Rep. 38(6):699-714. doi: 10.1007/s00299-019-02398-x.

661 Cheng H, Cai H, Fu H, An Z, Fang J, Hu Y, Guo D, Huang H. (2015). Functional Characterization of
662 Hevea brasiliensis CRT/DRE Binding Factor 1 Gene Revealed Regulation Potential in the

663 CBF Pathway of Tropical Perennial Tree. PLoS ONE 10(9): e0137634.
664 https://doi.org/10.1371/journal.pone.0137634

665 Cheng H, Chen X, Fang J, An Z, Hu Y, Huang H. (2018). Comparative transcriptome analysis
666 reveals an early gene expression profile that contributes to cold resistance in Hevea
667 brasiliensis (the Para rubber tree), Tree Physiology, Volume 38, Issue 9 Pages 1409–1423,
668 https://doi.org/10.1093/treephys/tpy014

669 Chini A, Fonseca S, Fernández G, Adie B, Chico J M, Lorenzo O, García-Casado G, López-Vidriero
670 I, Lozano F M, Ponce M R, Micol J L & Solano R. (2007). The JAZ family of repressors is the
671 missing link in jasmonate signaling. Nature volume 448, pages 666–671.

672 Dall'Osto L, Lico C, Alric J, Giuliano G, Havaux M, Bassi R. (2006). Lutein is needed for efficient
673 chlorophyll triplet quenching in the major LHCII antenna complex of higher plants and
674 effective photoprotection in vivo under strong light. BMC Plant Biol. 6:32. doi: 10.1186/1471-
675 2229-6-32.

676 Du, H., Liu, H., & Xiong, L. (2013). Endogenous auxin and jasmonic acid levels are differentially
677 modulated by abiotic stresses in rice. Frontiers in plant science, 4, 397.

678 de Faÿ, E., & Jacob, J. L. (1989). Anatomical organization of the laticiferous system in the bark. In
679 Physiology of rubber tree latex (pp. 3-14). CRC Press.

680 de Longevialle AF, Hendrickson L, Taylor NL, Delannoy E, Lurin C, Badger M, Millar AH, Small I.
681 (2008). The pentatricopeptide repeat gene OTP51 with two LAGLIDADG motifs is required
682 for the cis-splicing of plastid ycf3 intron 2 in Arabidopsis thaliana. Plant J. 56(1):157-68. doi:
683 10.1111/j.1365-313X.2008.03581.x.

684 den Broeck L V , Dubois M , Vermeersch M, Storme V , Matsui M, Inzé D. (2017). From network to
685 phenotype: the dynamic wiring of an Arabidopsis transcriptional network induced by osmotic
686 stress. Mol Syst Biol. 21;13(12):961. doi: 10.15252/msb.20177840.

687 Deng X, Wang J, Li Y, Wu S, Yang S, Chao J, Chen Y, Zhang S, Shi M, Tian W. (2018a). Comparative
688 transcriptome analysis reveals phytohormone signalings, heat shock module and ROS
689 scavenger mediate the cold-tolerance of rubber tree. Sci Rep. 8(1):4931. doi: 10.1038/s41598-
690 018-23094-y.

691 Deng, X., Guo, D., Yang, S., Shi, M., Chao, J., Li, H., et al., (2018b). Jasmonate signalling in
692 regulation of rubber biosynthesis in laticifer cells of rubber tree (Hevea brasiliensis muell.
693 arg.). J. Exp. Bot. 69, 3559–3571. doi: 10.1093/jxb/ery169

694 Ding, Z, Fu, L, Tan, D, Sun, X, Zhang, J. (2020). An integrative transcriptomic and genomic analysis
695 reveals novel insights into the hub genes and regulatory networks associated with rubber
696 synthesis in H. brasiliensis, Industrial Crops and Products, Volume 153, 112562

697 Dong J, Cao L, Zhang X, Zhang W, Yang T, Zhang J, Che D. (2021). An R2R3-MYB Transcription
698 Factor RmMYB108 Responds to Chilling Stress of Rosa multiflora and Conferred Cold

699 Tolerance of Arabidopsis. Front Plant Sci. 2021 Jul 27;12:696919. doi:
700 10.3389/fpls.2021.696919.

701 Dusa, A. (2017). *venn: Draw Venn Diagrams*. R package version 1.2. Available online at:
702 https://cran.microsoft.com/snapshot/2018-03-30/web/packages/venn/venn.pdf

703 Griffiths J, Murase K, Rieu I, Zentella R, Zhang ZL, Powers SJ, Gong F, Phillips AL, Hedden P, Sun
704 TP, Thomas SG. (2006). Genetic characterization and functional analysis of the GID1
705 gibberellin receptors in Arabidopsis. Plant Cell. 18(12):3399-414. doi:
706 10.1105/tpc.106.047415.

707 Gonçalves PS & Fontes JRA (2009) Domesticação e Melhoramento da Seringueira. In: BORÉM A,
708 LOPES MTG, CLEMENT CR & NODA H (Eds). Domesticação e Melhoramento: Espécies
709 Amazônicas. Viçosa: UFV, p.395-423.

710 Gong, XX., Yan, BY., Hu, J. et al., (2018). Transcriptome profiling of rubber tree (Hevea
711 brasiliensis) discovers candidate regulators of the cold stress response. Genes Genom 40,
712 1181–1197 https://doi.org/10.1007/s13258-018-0681-5

713 Harris MA, Clark J, Ireland A, Lomax J, Ashburner M, Foulger R, et al., The gene ontology (GO)
714 database and informatics resource. Nucleic Acids Res. 2004;32:D258–61.

715 Heitz T, Widemann E, Lugan R, Miesch L, Ullmann P, Désaubry L, Holder E, Grausem B, Kandel S,
716 Miesch M, Werck-Reichhart D, Pinot F. (2012). Cytochromes P450 CYP94C1 and CYP94B3
717 catalyze two successive oxidation steps of plant hormone Jasmonoyl-isoleucine for catabolic
718 turnover. J Biol Chem. 287(9):6296-306. doi: 10.1074/jbc.M111.316364.

719 International Rubber Consortium Limited (IRCo) https://ircorubber.com/2019/pestalotiopsis-
720 endanger-national-rubber-production/

721 Jiang J, Ma S, Ye N, Jiang M, Cao J, Zhang J. (2017). J Integr Plant Biol. WRKY transcription factors
722 in plant responses to stresses. 59(2):86-101. doi: 10.1111/jipb.12513.

723 Latrasse D, Benhamed M, Henry Y, Domenichini S, Kim W, Zhou D X, Delarue M. (2008). The MYST
724 histone acetyltransferases are essential for gametophyte development in Arabidopsis. BMC
725 Plant Biol. 28;8:121. doi: 10.1186/1471-2229-8-121.

726 Langfelder, P., Horvath, S. (2008). WGCNA: an R package for weighted correlation network
727 analysis. BMC Bioinformatics 9, 559. https://doi.org/10.1186/1471-2105-9-559

728 Koido, M., Tani, Y., Tsukahara, S., Okamoto, Y., & Tomida, A. (2018). InDePTH: detection of hub
729 genes for developing gene expression networks under anticancer drug treatment. Oncotarget,
730 9(49), 29097.

731 Mantello CC, Boatwright L, da Silva CC, Scaloppi EJ Jr, de Souza Goncalves P, Barbazuk WB,
732 Souza AP. (2019). Deep expression analysis reveals distinct cold-response strategies in rubber
733 tree (Hevea brasiliensis). BMC Genomics 20:455. https://doi.org/10.1186/s12864-019-5852-5

Min J H, Chung J S, Lee K H, Kim C S. (2014). The CONSTANS-like 4 transcription factor, AtCOL4, positively regulates abiotic stress tolerance through an abscisic acid-dependent manner in Arabidopsis. J Integr Plant Biol. 57(3):313-24. doi.org/10.1111/jipb.12246

Merico D, Isserlin R, Stueker O, Emili A, Bader GD PLoS One. (2010). Enrichment Map: A Network-Based Method for Gene-Set Enrichment Visualization and Interpretation Nov 15;5(11):e13984.

Müller M, Munné-Bosch S. (2015). Ethylene Response Factors: A Key Regulatory Hub in Hormone and Stress Signaling. Plant Physiol. 169(1):32-41. doi: 10.1104/pp.15.00677

Navari-Izzo F, Quartacci MF, Sgherri C. (2002). Lipoic acid: a unique antioxidant in the detoxification of activated oxygen species. Plant Physiol Biochem. 40:463–70.

Pata M O, Hannun Y A, Ng C K Y. (2010). Plant sphingolipids: decoding the enigma of the Sphinx. New Phytol. 185(3):611-30. doi: 10.1111/j.1469-8137.2009.03123.x.

Pootakham, W., Sonthirod, C., Naktang, C., Ruang-Areerate, P., Yoocha, T., Sangsrakru, D., ... & Tangphatsornruang, S. (2017). De novo hybrid assembly of the rubber tree genome reveals evidence of paleotetraploidy in Hevea species. Scientific reports, 7(1), 1-15.

Priyadarshan PM, Goncalves PS. *Hevea* gene pool for breeding. Genet Resour Crop Evol. 2003;50: 101–114.

Priyadarshan P.M. Hoa T.T.T. Huasun H. Gonc ̧alves P. de S. (2005) Yielding potential of rubber(Hevea brasiliensis) in sub-optimal environments. J. Crop Improv. 14, 221–247.

Priyadarshan. P. M. et al., Breeding Hevea Rubber. In: Jain, S.M.; Priyadarshan, P. M. (Ed.). Breeding Plantation Crops. Tropical Species, New York: Springer Science, 2009. p. 469-524.

Priyadarshan, P. M., & Clément-Demange, A. (2004). 3 Breeding Hevea Rubber: Formal and Molecular Genetics. *Advances in Genetics*, *52*, 51-116.

R Core Team (2020). R: A language and environment for statistical computing. R Foundation for Statistical Computing, Vienna, Austria. URL: https://www.R-project.org/.

Rivas-San Vicente, M., Larios-Zarate, G. & Plasencia, J. (2013). Disruption of sphingolipid biosynthesis in Nicotiana benthamiana activates salicylic acid-dependent responses and compromises resistance to Alternaria alternata f. sp. lycopersici . Planta 237, 121–136. https://doi.org/10.1007/s00425-012-1758-z

Robinson MD, McCarthy DJ, Smyth GK. edgeR: a Bioconductor package for differential expression analysis of digital gene expression data. Bioinformatics. 2010 Jan 1;26(1):139-40.

de Souza LM, Le Guen V, Cerqueira-Silva CBM, Silva CC, Mantello CC, et al., Genetic Diversity Strategy for the Management and Use of Rubber Genetic Resources: More than 1,000 Wild and Cultivated Accessions in a 100-Genotype Core Collection. PLOS ONE, v. 10, n. 8, p. 1-20, 2015.

769 Soitamo A J, Piippo M, Allahverdiyeva Y, Battchikova N, Aro E M. (2008). Light has a specific role
770 in modulating Arabidopsis gene expression at low temperature. BMC Plant Biol. 29;8:13. doi:
771 10.1186/1471-2229-8-13.

772 Steinbach Y. (2019). The Arabidopsis thaliana CONSTANS- LIKE 4 (COL4) - A Modulator of
773 Flowering Time. Front Plant Sci.28;10:651. doi: 10.3389/fpls.2019.00651.

774 Sun, S., Lin, M., Qi, X. et al., (2021). Full-length transcriptome profiling reveals insight into the cold
775 response of two kiwifruit genotypes (A. arguta) with contrasting freezing tolerances. BMC
776 Plant Biol 21, 365 https://doi.org/10.1186/s12870-021-03152-w

777 Tang X, Wang Q, Yuan H, Huang X. (2018). Chilling-induced DNA Demethylation is associated
778 with the cold tolerance of Hevea brasiliensis. BMC Plant Biol. 18(1):70. doi: 10.1186/s12870-
779 018-1276-7.

780 Theocharis, A., Clément, C., and Barka, E. A. (2012). Physiological and molecular changes in plants
781 grown at low temperatures. *Planta* 235, 1091–1105. doi: 10.1007/s00425-012-1641-y

782 Thines B, Katsir L, Melotto M, Niu Y, Mandaokar A, Liu G, Nomura K, He SY, Howe GA, Browse
783 J. (2007). JAZ repressor proteins are targets of the SCF(COI1) complex during jasmonate
784 signalling. Nature 448(7154):661-5. doi: 10.1038/nature05960.

785 Umer MJ, Bin Safdar L, Gebremeskel H, Zhao S, Yuan P, Zhu H, et al., (2020). Identification of key
786 gene networks controlling organic acid and sugar metabolism during watermelon fruit
787 development by integrating metabolic phenotypes and gene expression profiles. Hortic
788 Res.7(1):193. https://doi.org/10.1038/s41438-020-00416-8.

789 Widemann E, Miesch L, Lugan R, Holder E, Heinrich C, Aubert Y, Miesch M, Pinot F, Heitz T. (2013).
790 The amidohydrolases IAR3 and ILL6 contribute to jasmonoyl-isoleucine hormone turnover and
791 generate 12-hydroxyjasmonic acid upon wounding in Arabidopsis leaves. J Biol Chem.
792 288(44):31701-14. doi: 10.1074/jbc.M113.499228.

793 Xiao J, Zhang H, Xing L, Xu S, Liu H, Chong K, Xu Y. (2013). Requirement of histone
794 acetyltransferases HAM1 and HAM2 for epigenetic modification of FLC in regulating
795 flowering in Arabidopsis. J Plant Physiol.1;170(4):444-51. doi: 10.1016/j.jplph.2012.11.007.

796 Yang, H., Yang, S., Li, Y., & Hua, J. (2007). The Arabidopsis BAP1 and BAP2 genes are general
797 inhibitors of programmed cell death. Plant physiology, 145(1), 135–146.

798 Yuan H-M, Sheng Y, Chen W-J, Lu Y-Q, Tang X, Ou-Yang M, Huang X. (2017). Overexpression of
799 Hevea brasiliensis HbICE1 Enhances Cold Tolerance in Arabidopsis. Front Plant Sci. 8:1462.
800 doi: 10.3389/fpls.2017.01462.

801 Ye J W, Gong Z Y, Chen CG, Mi HL, Chen GY. (2012). A mutation of OSOTP 51 leads to
802 impairment of photosystem I complex assembly and serious photo-damage in rice. J Integr
803 Plant Biol.54(2):87-98. doi: 10.1111/j.1744-7909.

804

805 **Tables**

806 **Table 1**. Number of differentially expressed genes (DEGs) in *Hevea brasiliensis* that were modulated
807 by cold stress.

Time period comparison	**DEGs**	**Upregulated DEGs**	**Downregulated DEGs**
0h vs. 90m	32	32	0
0h vs. vs 12h	673	558	115
0h vs. 24h	1,208	852	356
90m vs. 12h	526	455	71
90m vs. 24h	917	700	217
12h vs. 24h	18	15	3
(0h + 90min) vs. (12h + 24h)	2,436	1,575	861

808

809 **Figure Legends**

810 **Figure 1**. (A) Principal component analysis (PCA) scatter plot performed on the first two principal
811 components (PCs) of rubber tree transcriptome data (GT1 and RRIM600 genotypes). Each point
812 represents a different sample, colored according to the respective genotype. (B) Venn diagrams of
813 differentially expressed genes (DEGs) detected under the established conditions.

814 **Figure 2**. (A) Gene coexpression network (CGN) modeled; Each node represents a gene, colored
815 according to the differential expression analysis results, and each connection has a minimum R
816 Pearson correlation coefficient of 0.8 (corrected with the highest reciprocal rank (HRR) approach).
817 (B) GCN network constructed according to the groups identified by the heuristic cluster chiseling
818 algorithm (HCCA); each node represents a cluster, colored according to the occurrence of
819 differentially expressed genes (DEGs).

820 **Figure 3**. (A) Gene coexpression network (CGN) modeled; Each node represents a gene, colored
821 according to the Gene Ontology (GO) enrichment term found in the related cluster, and each
822 connection has a minimum R Pearson correlation coefficient of 0.8 (corrected with the highest
823 reciprocal rank (HRR) approach). (B) GCN network constructed according to the groups identified
824 by the heuristic cluster chiseling algorithm (HCCA); each node represents a cluster, colored
825 according to GO enrichment term.

826 Figure 4. Gene Ontology (GO) terms for the cold response modules selected: (A) Upregulated
827 modules; (B) Downregulated modules.

828 Supplementary Figure 1. (A) Gene coexpression network (GCN), colored according to the modules
829 considered associated with the cold response; each node represents a gene, and each connection has a
830 minimum R Pearson correlation coefficient of 0.8 (corrected with the highest reciprocal rank (HRR)
831 approach). (B) GCN network constructed according to the groups identified by the heuristic cluster
832 chiseling algorithm (HCCA); each node represents a cluster, colored according to modules selected
833 and sized according to the proportion of DEGs (Supplementary Table 5).

834

835

836

837

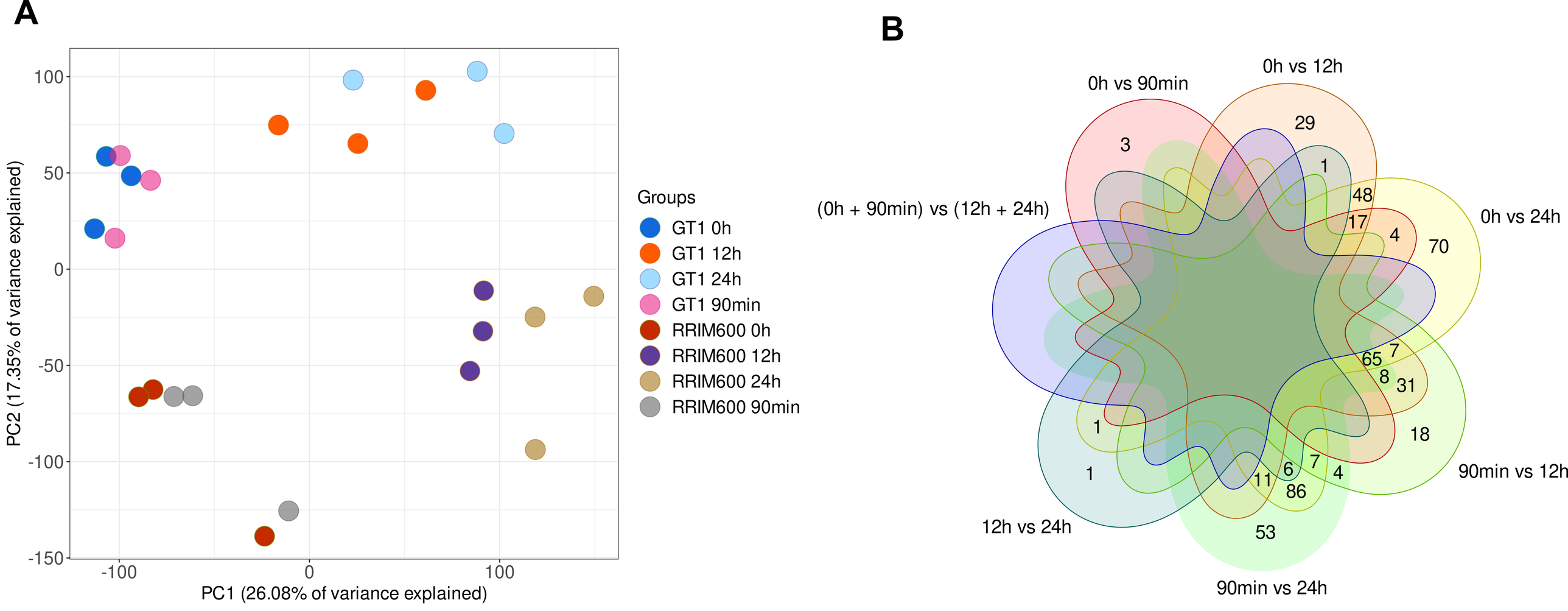
A
100
50
0
-50
-100
-150
-100
0
100
PC2 (17.35% of variance explained)
PC1 (26.08% of variance explained)
Groups
GT1 0h
GT1 12h
GT1 24h
GT1 90min
RRIM600 0h
RRIM600 12h
RRIM600 24h
RRIM600 90min
B
0h vs 90min
0h vs 12h
(0h + 90min) vs (12h + 24h)
0h vs 24h
90min vs 12h
12h vs 24h
90min vs 24h
3
29
1
48
17
4
70
65
7
8
31
18
1
1
7
4
6
11
86
53

A

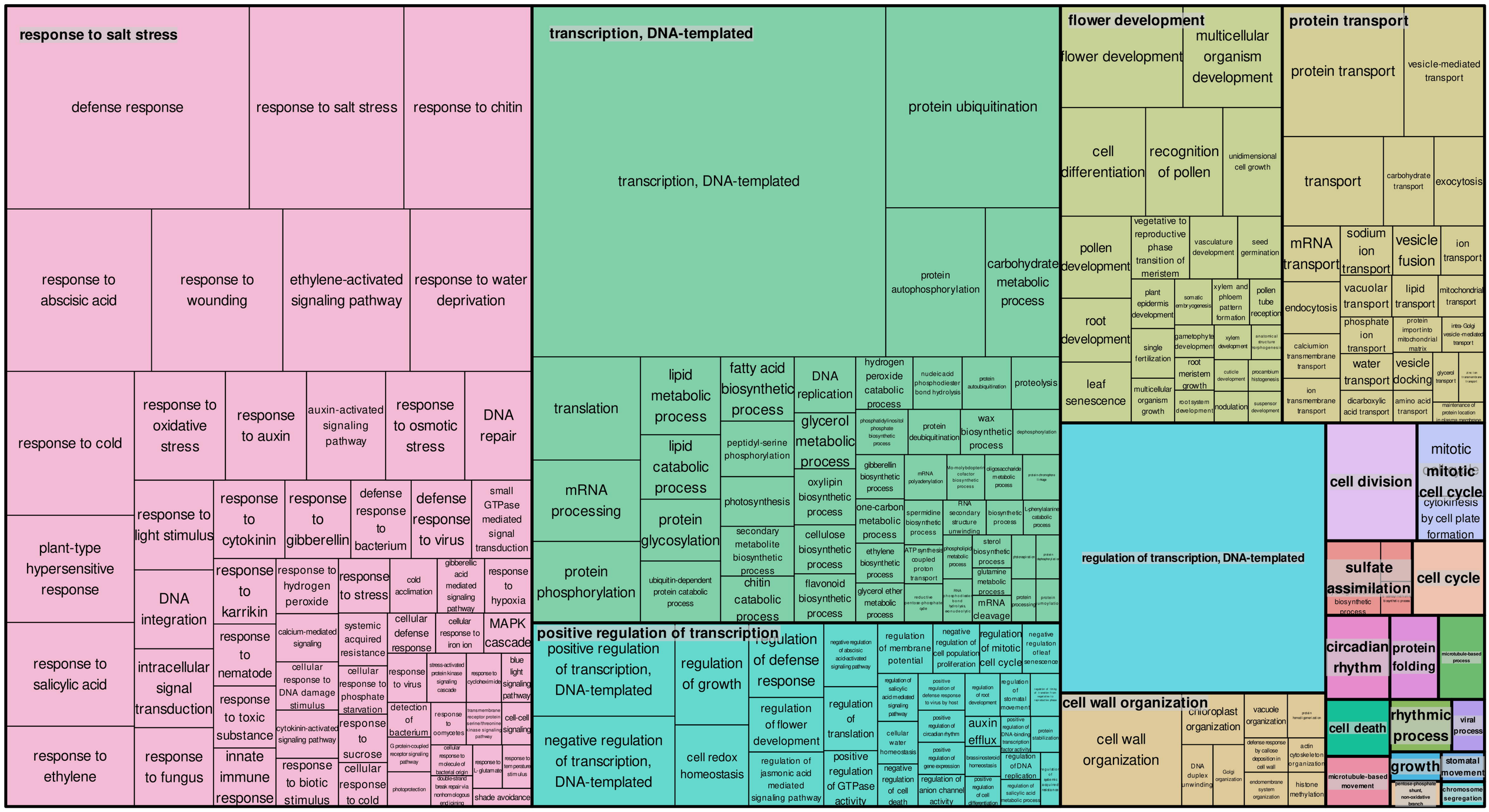
response to salt stress
defense response
response to salt stress
response to chitin
response to abscisic acid
response to wounding
ethylene-activated signaling pathway
response to water deprivation
response to cold
response to oxidative stress
response to auxin
auxin-activated signaling pathway
response to osmotic stress
DNA repair
plant-type hypersensitive response
response to light stimulus
response to cytokinin
response to gibberellin
defense response to bacterium
defense response to virus
small GTPase mediated signal transduction
DNA integration
response to karrikin
response to hydrogen peroxide
response to stress
cold acclimation
gibberellic acid mediated signaling pathway
response to hypoxia
response to salicylic acid
response to nematode
calcium-mediated signaling
systemic acquired resistance
cellular defense response
cellular response to iron ion
MAPK cascade
intracellular signal transduction
cellular response to DNA damage stimulus
cellular response to phosphate starvation
response to virus
stress-activated protein kinase signaling cascade
response to cycloheximide
blue light signaling pathway
response to toxic substance
cytokinin-activated signaling pathway
detection of bacterium
response to oomycetes
transmembrane receptor protein serine/threonine kinase signaling pathway
cell-cell signaling
response to ethylene
response to fungus
innate immune response
response to biotic stimulus
response to sucrose
G protein-coupled receptor signaling pathway
cellular response to molecule of bacterial origin
response to L-glutamate
response to temperature stimulus
cellular response to cold
photoprotection
double-strand break repair via nonhomologous end-joining
shade avoidance
transcription, DNA-templated
transcription, DNA-templated
protein ubiquitination
protein autophosphorylation
carbohydrate metabolic process
translation
lipid metabolic process
fatty acid biosynthetic process
DNA replication
hydrogen peroxide catabolic process
nucleic acid phosphodiester bond hydrolysis
protein autoubiquitination
proteolysis
mRNA processing
lipid catabolic process
peptidyl-serine phosphorylation
glycerol metabolic process
phosphatidylinositol phosphate biosynthetic process
protein deubiquitination
wax biosynthetic process
dephosphorylation
protein phosphorylation
protein glycosylation
photosynthesis
oxylipin biosynthetic process
gibberellin biosynthetic process
mRNA polyadenylation
Mo-molybdopterin cofactor biosynthetic process
oligosaccharide metabolic process
protein-chromophore linkage
one-carbon metabolic process
spermidine biosynthetic process
RNA secondary structure unwinding
biosynthetic process
L-phenylalanine catabolic process
secondary metabolite biosynthetic process
cellulose biosynthetic process
ethylene biosynthetic process
ATP synthesis coupled proton transport
phospholipid metabolic process
sterol biosynthetic process
photorespiration
protein lipoylation
glutamine metabolic process
ubiquitin-dependent protein catabolic process
chitin catabolic process
flavonoid biosynthetic process
glycerol ether metabolic process
reductive pentose-phosphate cycle
RNA phosphodiester bond hydrolysis, endonucleolytic
mRNA cleavage
protein processing
protein homodimerization
positive regulation of transcription
positive regulation of transcription, DNA-templated
regulation of growth
regulation of defense response
negative regulation of abscisic acid-activated signaling pathway
regulation of membrane potential
negative regulation of cell population proliferation
regulation of mitotic cell cycle
negative regulation of leaf senescence
negative regulation of transcription, DNA-templated
cell redox homeostasis
regulation of flower development
regulation of translation
regulation of salicylic acid mediated signaling pathway
positive regulation of defense response to virus by host
regulation of root development
regulation of stomatal movement
regulation of jasmonic acid mediated signaling pathway
positive regulation of GTPase activity
cellular water homeostasis
positive regulation of circadian rhythm
auxin efflux
positive regulation of DNA-binding transcription factor activity
protein stabilization
negative regulation of cell death
positive regulation of gene expression
brassinosteroid homeostasis
regulation of DNA replication
regulation of anion channel activity
positive regulation of cell differentiation
regulation of salicylic acid metabolic process
flower development
flower development
multicellular organism development
cell differentiation
recognition of pollen
unidimensional cell growth
pollen development
vegetative to reproductive phase transition of meristem
vasculature development
seed germination
plant epidermis development
somatic embryogenesis
xylem and phloem pattern formation
pollen tube reception
root development
single fertilization
gametophyte development
xylem development
anatomical structure morphogenesis
leaf senescence
root meristem growth
cuticle development
procambium histogenesis
multicellular organism growth
root system development
nodulation
suspensor development
protein transport
protein transport
vesicle-mediated transport
transport
carbohydrate transport
exocytosis
mRNA transport
sodium ion transport
vesicle fusion
ion transport
endocytosis
vacuolar transport
lipid transport
mitochondrial transport
phosphate ion transport
protein import into mitochondrial matrix
intra-Golgi vesicle-mediated transport
calcium ion transmembrane transport
water transport
vesicle docking
glycerol transport
zinc ion transmembrane transport
ion transmembrane transport
dicarboxylic acid transport
amino acid transport
maintenance of protein location in plasma membrane
regulation of transcription, DNA-templated
cell division
mitotic cell cycle
mitotic cell cycle
cytokinesis by cell plate formation
sulfate assimilation
biosynthetic process
cell cycle
circadian rhythm
protein folding
microtubule-based process
cell wall organization
cell wall organization
chloroplast organization
vacuole organization
protein homodimerization
cell death
rhythmic process
viral process
DNA duplex unwinding
Golgi organization
defense response by callose deposition in cell wall
actin cytoskeleton organization
microtubule-based movement
endomembrane system organization
histone methylation
growth
stomatal movement
pentose-phosphate shunt, non-oxidative branch
chromosome segregation

B

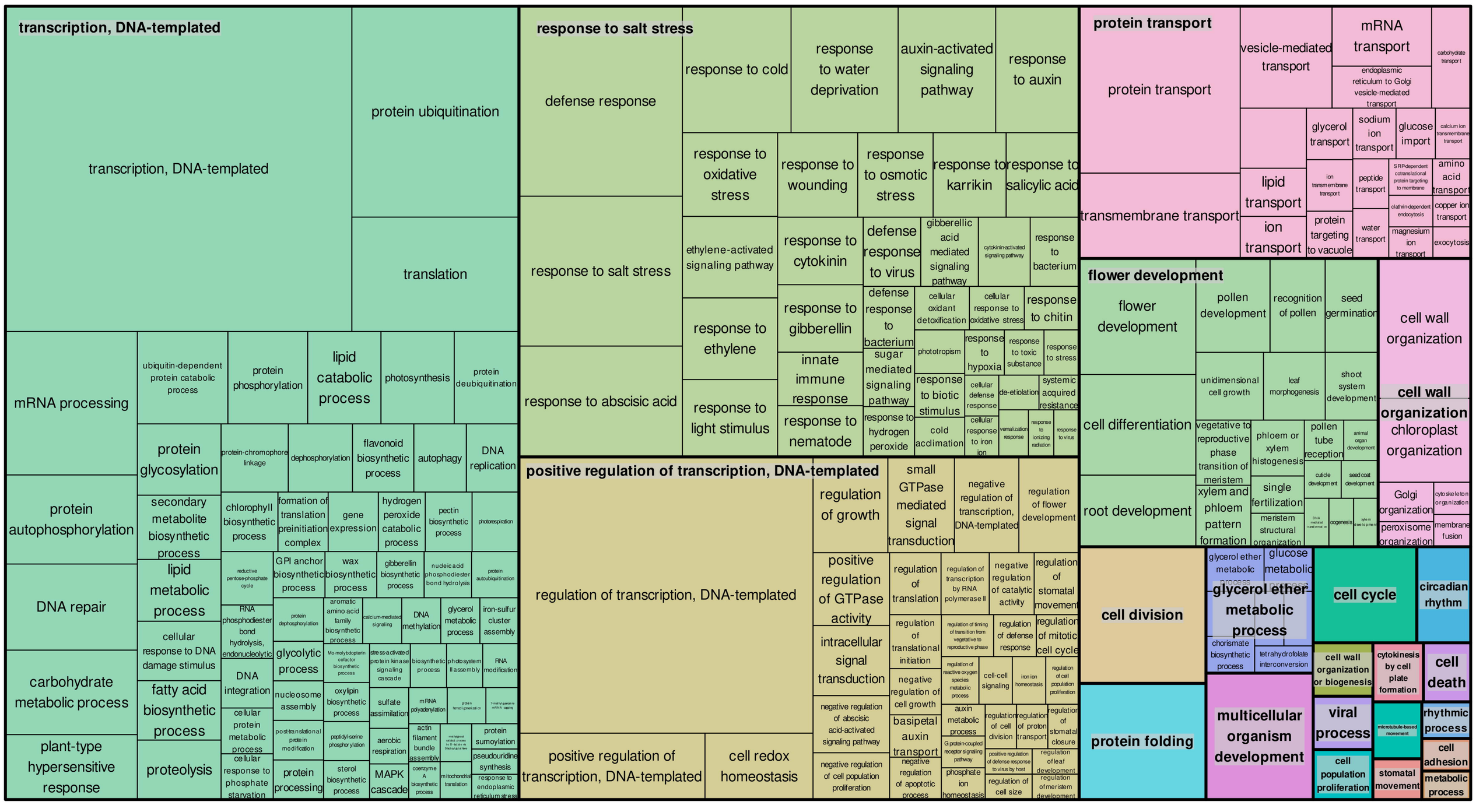
transcription, DNA-templated
transcription, DNA-templated
protein ubiquitination
translation
mRNA processing
ubiquitin-dependent protein catabolic process
protein phosphorylation
lipid catabolic process
photosynthesis
protein deubiquitination
protein autophosphorylation
protein glycosylation
protein-chromophore linkage
dephosphorylation
flavonoid biosynthetic process
autophagy
DNA replication
secondary metabolite biosynthetic process
chlorophyll biosynthetic process
formation of translation preinitiation complex
gene expression
hydrogen peroxide catabolic process
pectin biosynthetic process
photorespiration
lipid metabolic process
reductive pentose-phosphate cycle
GPI anchor biosynthetic process
wax biosynthetic process
gibberellin biosynthetic process
nucleic acid phosphodiester bond hydrolysis
protein autoubiquitination
DNA repair
RNA phosphodiester bond hydrolysis, endonucleolytic
protein dephosphorylation
aromatic amino acid family biosynthetic process
calcium-mediated signaling
DNA methylation
glycerol metabolic process
iron-sulfur cluster assembly
cellular response to DNA damage stimulus
glycolytic process
Mo-molybdopterin cofactor biosynthetic process
stress-activated protein kinase signaling cascade
biosynthetic process
photosystem II assembly
RNA modification
carbohydrate metabolic process
DNA integration
nucleosome assembly
oxylipin biosynthetic process
sulfate assimilation
mRNA polyadenylation
protein homodimerization
7-methylguanosine mRNA capping
fatty acid biosynthetic process
cellular protein metabolic process
post-translational protein modification
peptidyl-serine phosphorylation
aerobic respiration
actin filament bundle assembly
methylglyoxal catabolic process to D-lactate via S-lactoylglutathione
protein sumoylation
pseudouridine synthesis
plant-type hypersensitive response
proteolysis
cellular response to phosphate starvation
protein processing
sterol biosynthetic process
MAPK cascade
coenzyme A biosynthetic process
mitochondrial translation
response to endoplasmic reticulum stress
response to salt stress
defense response
response to cold
response to water deprivation
auxin-activated signaling pathway
response to auxin
response to salt stress
response to oxidative stress
response to wounding
response to osmotic stress
response to karrikin
response to salicylic acid
ethylene-activated signaling pathway
response to cytokinin
defense response to virus
gibberellic acid mediated signaling pathway
cytokinin-activated signaling pathway
response to bacterium
response to abscisic acid
response to ethylene
response to gibberellin
defense response to bacterium
cellular oxidant detoxification
cellular response to oxidative stress
response to chitin
phototropism
response to hypoxia
response to toxic substance
response to stress
innate immune response
sugar mediated signaling pathway
response to light stimulus
response to biotic stimulus
cellular defense response
de-etiolation
systemic acquired resistance
response to nematode
response to hydrogen peroxide
cold acclimation
cellular response to iron ion
vernalization response
response to ionizing radiation
response to virus
positive regulation of transcription, DNA-templated
regulation of growth
small GTPase mediated signal transduction
negative regulation of transcription, DNA-templated
regulation of flower development
regulation of transcription, DNA-templated
positive regulation of GTPase activity
regulation of translation
regulation of transcription by RNA polymerase II
negative regulation of catalytic activity
regulation of stomatal movement
intracellular signal transduction
regulation of translational initiation
regulation of timing of transition from vegetative to reproductive phase
regulation of defense response
regulation of mitotic cell cycle
negative regulation of cell growth
regulation of reactive oxygen species metabolic process
cell-cell signaling
iron ion homeostasis
regulation of cell population proliferation
negative regulation of abscisic acid-activated signaling pathway
basipetal auxin transport
auxin metabolic process
regulation of cell division
regulation of proton transport
regulation of stomatal closure
positive regulation of transcription, DNA-templated
cell redox homeostasis
negative regulation of cell population proliferation
negative regulation of apoptotic process
G protein-coupled receptor signaling pathway
positive regulation of defense response to virus by host
regulation of leaf development
phosphate ion homeostasis
regulation of cell size
regulation of meristem development
protein transport
protein transport
vesicle-mediated transport
mRNA transport
endoplasmic reticulum to Golgi vesicle-mediated transport
carbohydrate transport
glycerol transport
sodium ion transport
glucose import
calcium ion transmembrane transport
lipid transport
ion transmembrane transport
peptide transport
SRP-dependent cotranslational protein targeting to membrane
amino acid transport
transmembrane transport
protein targeting to vacuole
water transport
clathrin-dependent endocytosis
copper ion transport
ion transport
magnesium ion transport
exocytosis
flower development
flower development
pollen development
recognition of pollen
seed germination
cell wall organization
unidimensional cell growth
leaf morphogenesis
shoot system development
cell wall organization
cell differentiation
vegetative to reproductive phase transition of meristem
phloem or xylem histogenesis
pollen tube reception
animal organ development
chloroplast organization
root development
xylem and phloem pattern formation
single fertilization
cuticle development
seed coat development
meristem structural organization
DNA-mediated transformation
oogenesis
xylem development
Golgi organization
cytoskeleton organization
peroxisome organization
membrane fusion
cell division
glycerol ether metabolic process
glucose metabolic process
cell cycle
circadian rhythm
chorismate biosynthetic process
tetrahydrofolate interconversion
cell wall organization or biogenesis
cytokinesis by cell plate formation
cell death
protein folding
multicellular organism development
viral process
microtubule-based movement
rhythmic process
cell adhesion
cell population proliferation
stomatal movement
metabolic process

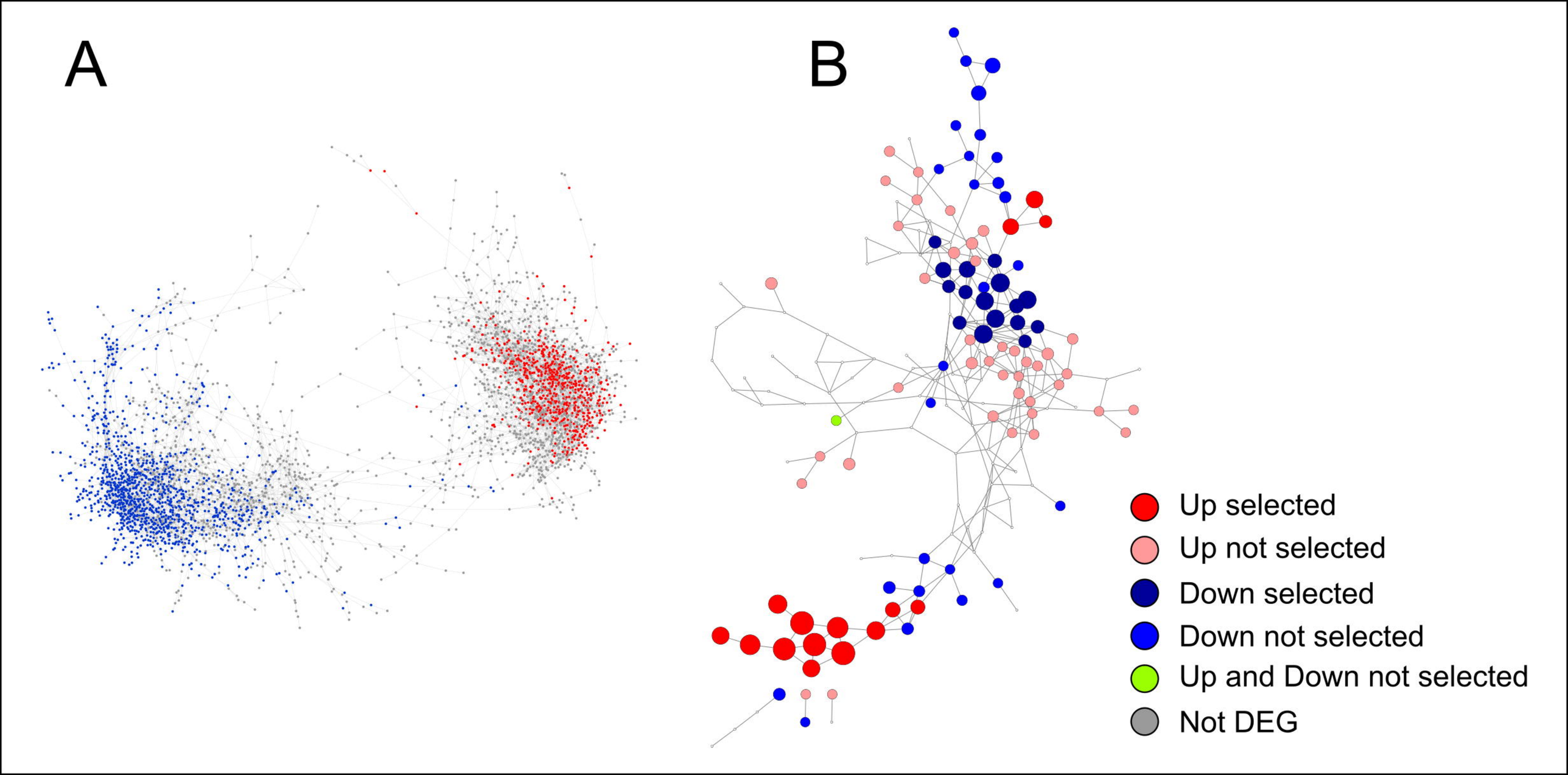
A
B
Up selected
Up not selected
Down selected
Down not selected
Up and Down not selected
Not DEG

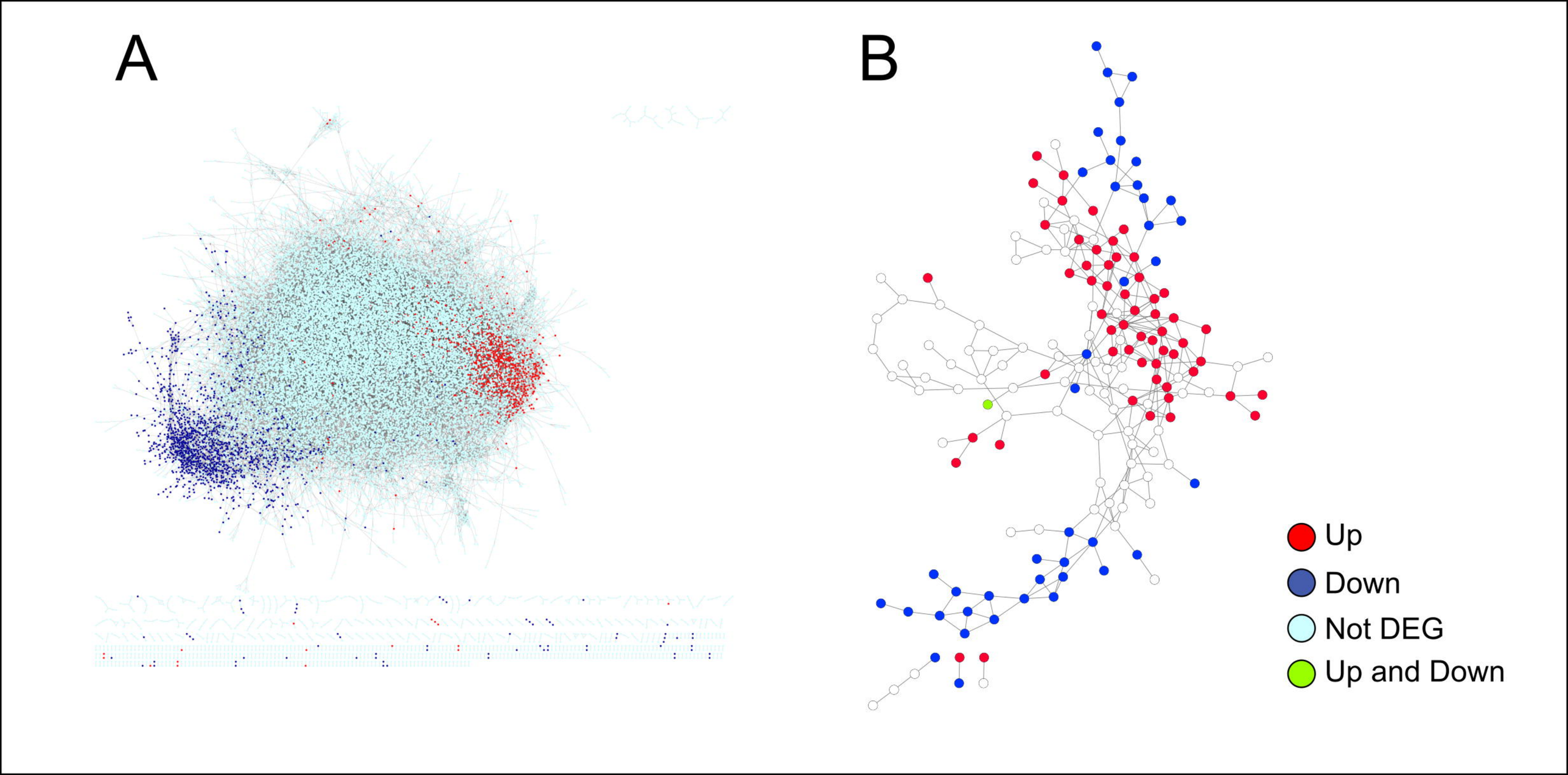
A
B
Up
Down
Not DEG
Up and Down

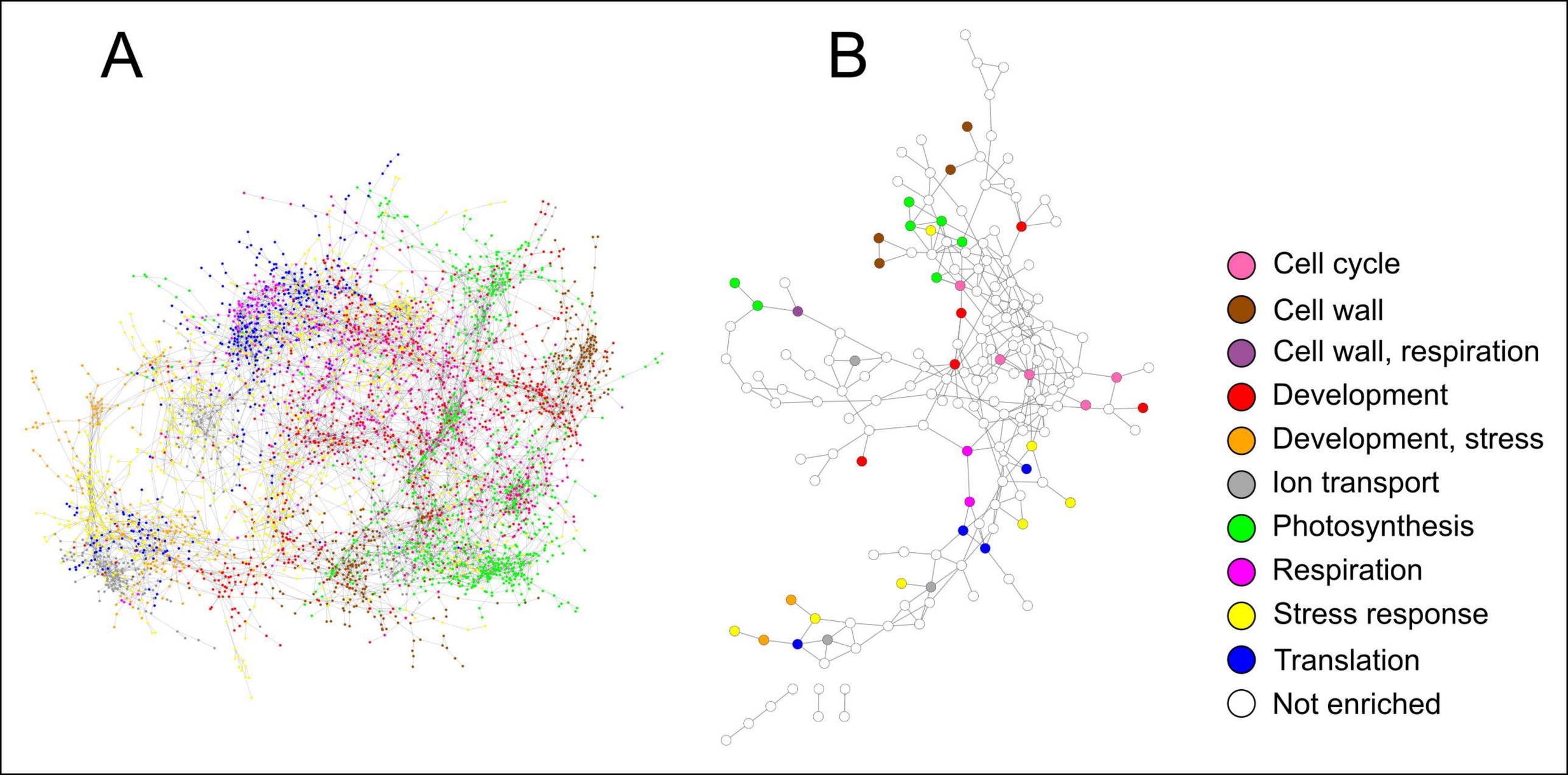
A
B
Cell cycle
Cell wall
Cell wall, respiration
Development
Development, stress
Ion transport
Photosynthesis
Respiration
Stress response
Translation
Not enriched